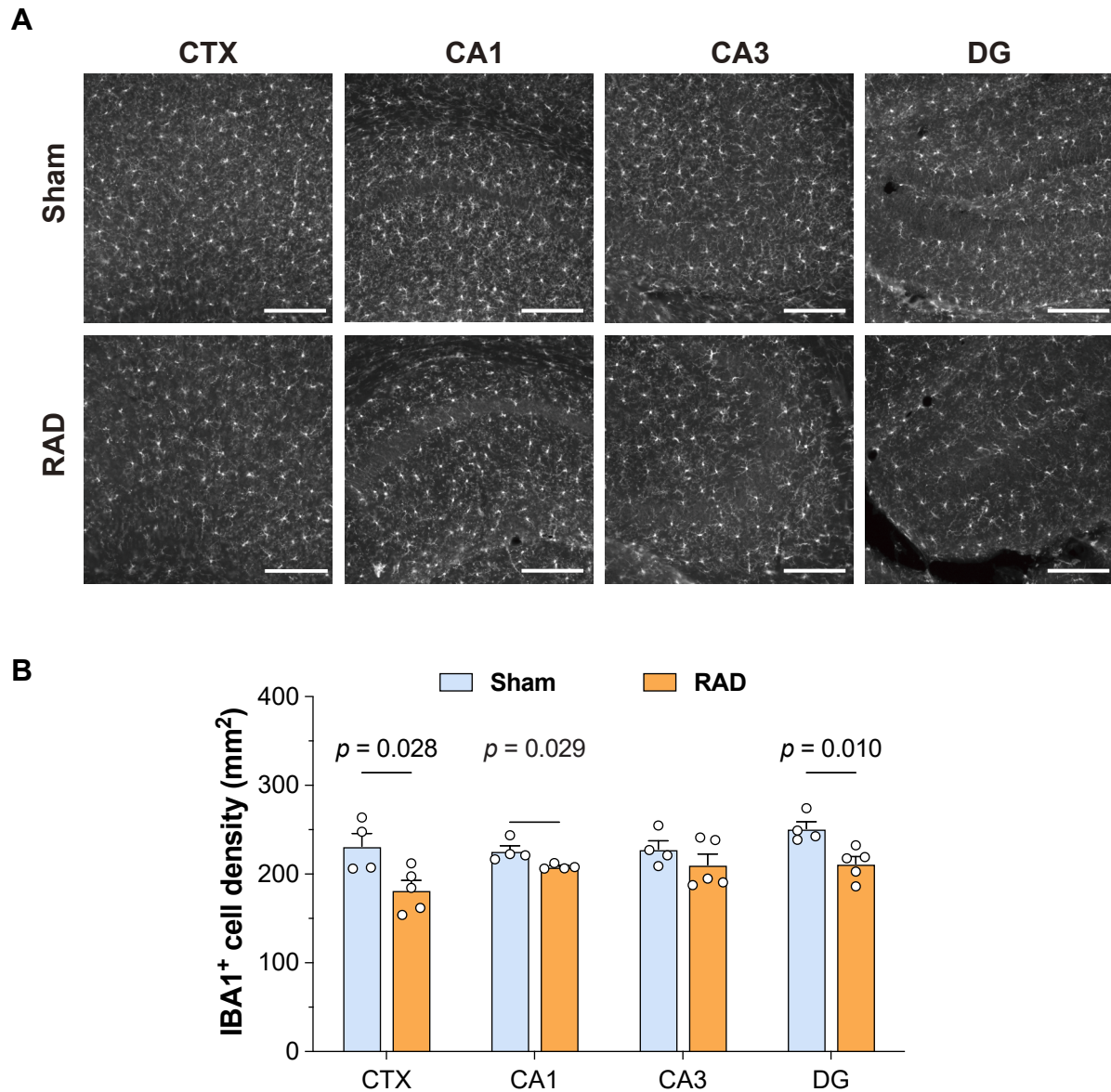
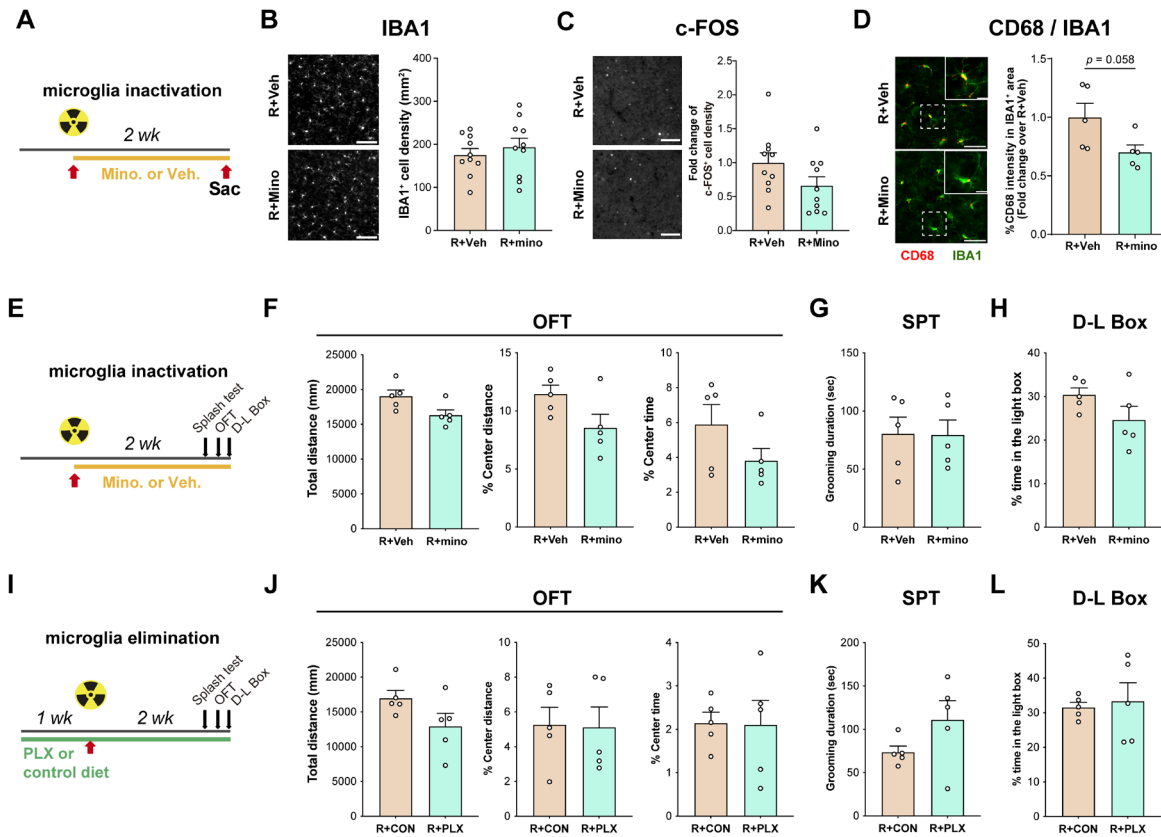


Supplementary Figure 1. Cranial irradiation-induced neuronal hypoactivity in the mPFC correlates to anxiety-like behaviors and is independent of neuronal loss. (A) Representative images of c-FOS immunostaining in the anterior cingulate cortex (ACC), lateral bed nucleus of stria terminalis (lBST), insular cortex (IC), lateral hypothalamus (LH), paraventricular thalamus (PVT), cornu ammonis 3 (CA3) and dentate gyrus (DG) of the dorsal hippocampus. Sham: mice without cranial irradiation, RAD: mice received cranial irradiation for two weeks. Scale bar: 200 μ m. (B) Correlation of anxiety-like behavioral indexes with the density of c-FOS positive cells in different brain regions with significantly altered neuronal activity. (C-D) Representative images of NeuN-positive cells (C), and quantification of NeuN-positive neurons in the mPFC. Sham: n=6; RAD: n=9. Data were represented as mean \pm s.e.m. and analyzed by Student's *t* test. Scale bar: 100 μ m. (E) Representative images of co-localization of c-FOS-positive (green) and CaMKII-positive excitatory neurons (red) in the mPFC of Sham and RAD groups. Scale bar: 50 μ m. (F) Representative images of co-localization of c-FOS-positive (green) and GAD67-positive inhibitory neurons (red) in the mPFC of Sham and RAD groups. Scale bar: 50 μ m. (G) Percentage of c-FOS-positive cells which were also GAD67-negative (GAD67⁻) or GAD67-positive (GAD67⁺) cells in the mPFC. Data are presented as mean percentage of c-FOS-positive cells.

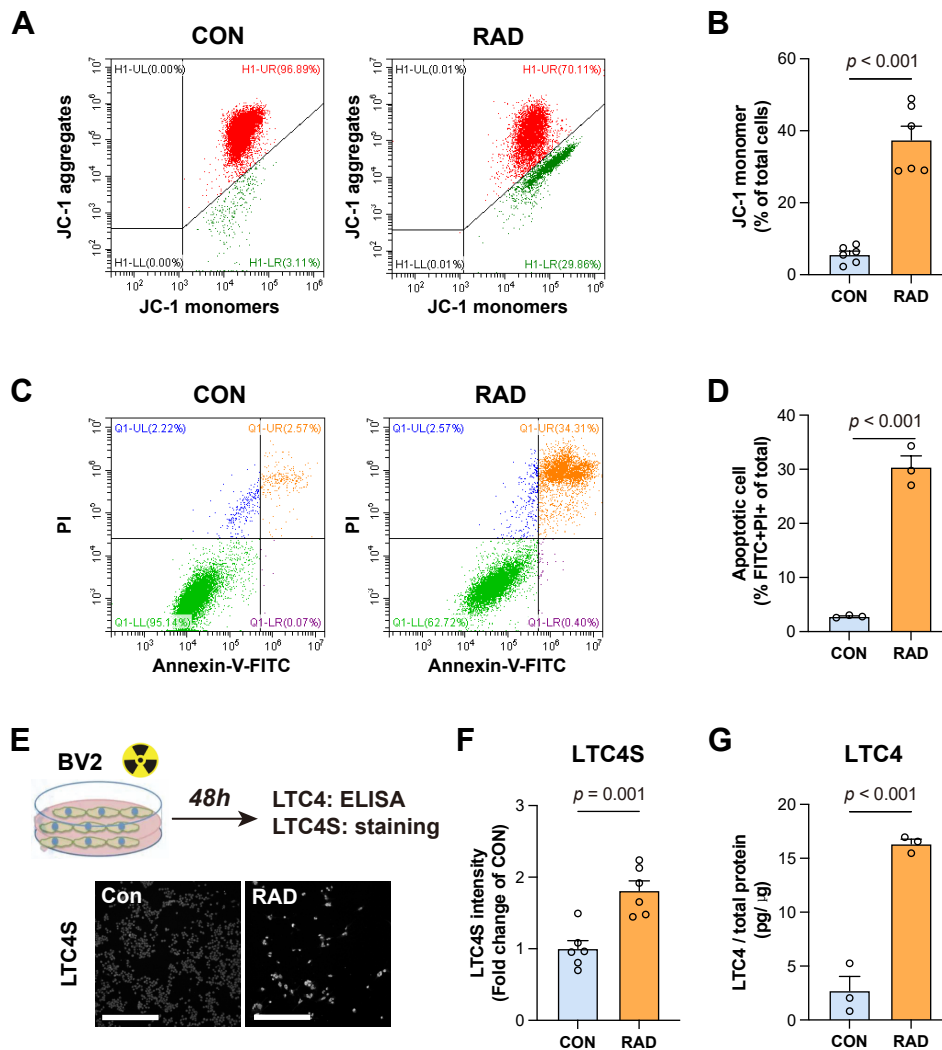


Supplementary Figure 2. Cranial irradiation reduces microglial cell density in the dorsal hippocampus and somatosensory cortex. (A) Representative images of IBA1-positive cells in the somatosensory cortex (CTX), cornu ammonis 1 (CA1), cornu ammonis 3 (CA3) and dentate gyrus (DG) of the dorsal hippocampus in the Sham and RAD groups. Scale bar: 200 μ m. (B) Quantification of the IBA1-positive cell density in the somatosensory cortex and hippocampal subregions (Sham: $n = 4$; RAD: $n = 4-5$). Data are presented as mean \pm s.e.m. and analyzed by multiple t tests.



Supplementary Figure 3. Minocycline treatment or continuous microglial depletion fails to ameliorate radiation-induced microglial loss, neuronal hypoactivity in the mPFC, and behavioral deficits. (A) Schematic of the experimental designs. Minocycline (R+mino, 30mg/kg, *i.p.*) or vehicle (R+Veh) was continuously administered post-irradiation. Tissue harvest (Sac) was conducted at 2 weeks (2 wk) post irradiation. (B) Representative images (left panel) and quantification (right panel) of IBA1-positive microglial cell density in the mPFC. Scale bar: 100µm. (C) Representative images (left panel) and quantification (right panel) of c-FOS-positive cell density in the mPFC. Scale bar: 100µm. (D) Representative images of CD68 (red) and IBA1 (green) immunostaining

and quantification of CD68 intensity in IBA1+ area of microglia cells in the mPFC. Scale bar, large image: 40 μ m, small image: 10 μ m. **(E)** Schematic of the experimental designs. Minocycline (R+mino) or vehicle (R+Veh) was continuously administered post-irradiation. Behavioral tests were conducted at 2 weeks (2 wk) post irradiation. **(F, J)** Quantification of total distance travelled, percentage of the time spent in center zone, and travelled distance in center zone as a percentage of the total distance in the open field test. **(G, K)** Quantification of the grooming duration during the splash test. **(H, L)** Quantification of time spend in the light box as a percentage of the total time in the D-L Box. **(B-C)**: R+Veh: n=10; R+mino: n=10. **(D, F-H)**: R+Veh: n=5; R+mino: n=5. **(I)** Schematic of the microglia-depletion experiment. Microglia were depleted by continuous administration of PLX3397-containing diet for 3 weeks, started 1 week before 15 Gy cranial irradiation (R+PLX). As a control, mice receiving 15 Gy irradiation were fed with regular chow diet throughout the whole experiment (R+CON). Behavioral tests and tissue harvest (Sac) were conducted at 2 weeks (2 wk) post irradiation. **(J-L)**: R+CON: n=5; R+PLX: n=5. Data are represented as mean \pm s.e.m. and analyzed by student's *t* test **(B-D, F-H, J-L)**.



Supplementary Figure 4. Radiation increases cell apoptosis, LTC4S expression, and LTC4 levels in the BV2 microglial cells. (A) Gating strategy and representative plots of JC-1 aggregates and monomers from flow cytometry analysis, measuring mitochondrial membrane potential of BV2 microglial cells from non-irradiated group (CON) and 10 Gy irradiated group (RAD). (B) Quantification of JC-1 monomers as the percentage of total cells (CON: n=6; RAD: n=6). (C) Gating strategy and representative plots of Annexin-V-FITC/PI flow cytometry analysis of BV2 microglial cells of non-irradiated group (CON) and 10 Gy irradiated group (RAD). Apoptotic cells (Annexin-V-FITC⁺ and PI⁺) were presented in upper right quadrant. (D) Quantification of apoptotic cells (Annexin-V-FITC⁺ and PI⁺) of total cells (CON: n=3; RAD: n=3). (E) Upper panel: schematic of the experimental designs. Lower panel: representative images of LTC4S staining of BV2 microglia cells from non-irradiated group (CON) and 10 Gy irradiated group (RAD). Scale bar: 300μm. (F) Quantification of LTC4S fluorescent intensity in irradiated BV2 microglial cells (RAD), compare to non-irradiated (CON) group (CON: n=6; RAD: n=6). (G) Quantification of the LTC4 levels in BV2 microglial cells between groups (CON: n=3; RAD: n=3). Data are represented as mean ± s.e.m. and analyzed by Student's *t* test.